



Additional Role of Nicotinic Acid Hydroxylase for the Transformation of 3-Succinoyl-Pyridine by *Pseudomonas* sp. Strain JY-Q

Jun Li,^a Shanshan Li,^a Linlin Xie,^a Guoqing Chen,^a Mingjie Shen,^a Fanda Pan,^b Ming Shu,^b Yang Yang,^b Yang Jiao,^c Fuming Zhang,^d Robert J. Linhardt,^d  Weihong Zhong^a

^aCollege of Biotechnology and Bioengineering, Zhejiang University of Technology, Hangzhou, China

^bTechnology Center, China Tobacco Zhejiang Industrial Co., Ltd., Hangzhou, China

^cTechnology Center, Hangzhou Liqueur Environmental Protection Paper Co., Ltd., Hangzhou, China

^dDepartment of Chemical and Biological Engineering, Center for Biotechnology and Interdisciplinary Studies, Rensselaer Polytechnic Institute, Troy, New York, USA

ABSTRACT Nicotine and nicotinic acid (NA) are both considered to be representatives of *N*-heterocyclic aromatic compounds, and their degradation pathways have been revealed in *Pseudomonas* species. However, the cooccurrence of these two pathways has only been observed in *Pseudomonas* sp. strain JY-Q. The nicotine pyrrolidine catabolism pathway of strain JY-Q consists of the functional modules Nic1, Spm, and Nic2. The module enzyme, 3-succinoylpyridine monooxygenase (Spm), catalyzes transformation of 3-succinoyl-pyridine (SP) to 6-hydroxy-3-succinoyl-pyridine (HSP). There exist two homologous but not identical Spm enzymes (namely, Spm1 and Spm2) in JY-Q. However, when *spm1* and *spm2* were both in-frame deleted, the mutant still grew well in basic salt medium (BSM) supplemented with nicotine as the sole carbon/nitrogen nutrition, suggesting that there exists an alternative pathway responsible for SP catabolism in JY-Q. NicAB, an enzyme accounting for NA hydroxylation, contains reorganized domains similar to those of Spm. When the JY-Q *nicAB* gene (*nicAB* in strain JY-Q) was introduced into another *Pseudomonas* strain, one that is unable to degrade NA, the resultant recombinant strain exhibited the ability to transform SP to HSP, but without the ability to metabolize NA. Here, we conclude that NicAB in strain JY-Q exhibits an additional role in SP transformation. The other genes in the NA cluster, NicXDFE (Nic2 homolog), then also exhibit a role in subsequent HSP metabolism for energy yield. This finding also suggests that the cooccurrence of nicotine and NA degradation genes in strain JY-Q represents an advantage for JY-Q, making it more effective and flexible for the degradation of nicotine.

IMPORTANCE 3-Succinoyl-pyridine (SP) and 6-hydroxy-3-succinoyl-pyridine (HSP) are both valuable chemical precursors to produce insecticides and hypotensive agents. SP and HSP could be renewable through the nicotine microbial degradation pathway, in which 3-succinoylpyridine monooxygenases (Spm) account for transforming SP into HSP in *Pseudomonas* sp. strain JY-Q. However, when two homologous Spm genes (*spm1* and *spm2*) were knocked out, the mutant retained the ability to degrade nicotine. Thus, in addition to Spm, JY-Q should have an alternative pathway for SP conversion. In this research, we showed that JY-Q_NicAB was responsible for this alternative SP conversion. Both of the primary functions for nicotinic acid dehydrogenation and the additional function for SP metabolism were detected in a recombinant strain harboring JY-Q_NicAB. As a result, both nicotinic acid and nicotine degradation pathways in JY-Q contribute to its remarkable nicotine tolerance and nicotine degradation availability. These findings also provide one more metabolic engineering strategy for accumulation for value-added intermediates.

Citation Li J, Li S, Xie L, Chen G, Shen M, Pan F, Shu M, Yang Y, Jiao Y, Zhang F, Linhardt RJ, Zhong W. 2021. Additional role of nicotinic acid hydroxylase for the transformation of 3-succinoyl-pyridine by *Pseudomonas* sp. strain JY-Q. *Appl Environ Microbiol* 87:e02740-20. <https://doi.org/10.1128/AEM.02740-20>.

Editor Haruyuki Atomi, Kyoto University

Copyright © 2021 American Society for Microbiology. All Rights Reserved.

Address correspondence to Yang Yang, Yangy@zjtobacco.com, or Weihong Zhong, whzhong@zjut.edu.cn.

Received 8 November 2020

Accepted 13 December 2020

Accepted manuscript posted online 4 January 2021

Published 26 February 2021

KEYWORDS *Pseudomonas* sp. strain JY-Q, nicotine, nicotinic acid, nicotinic acid hydroxylase, succinoyl-pyridine

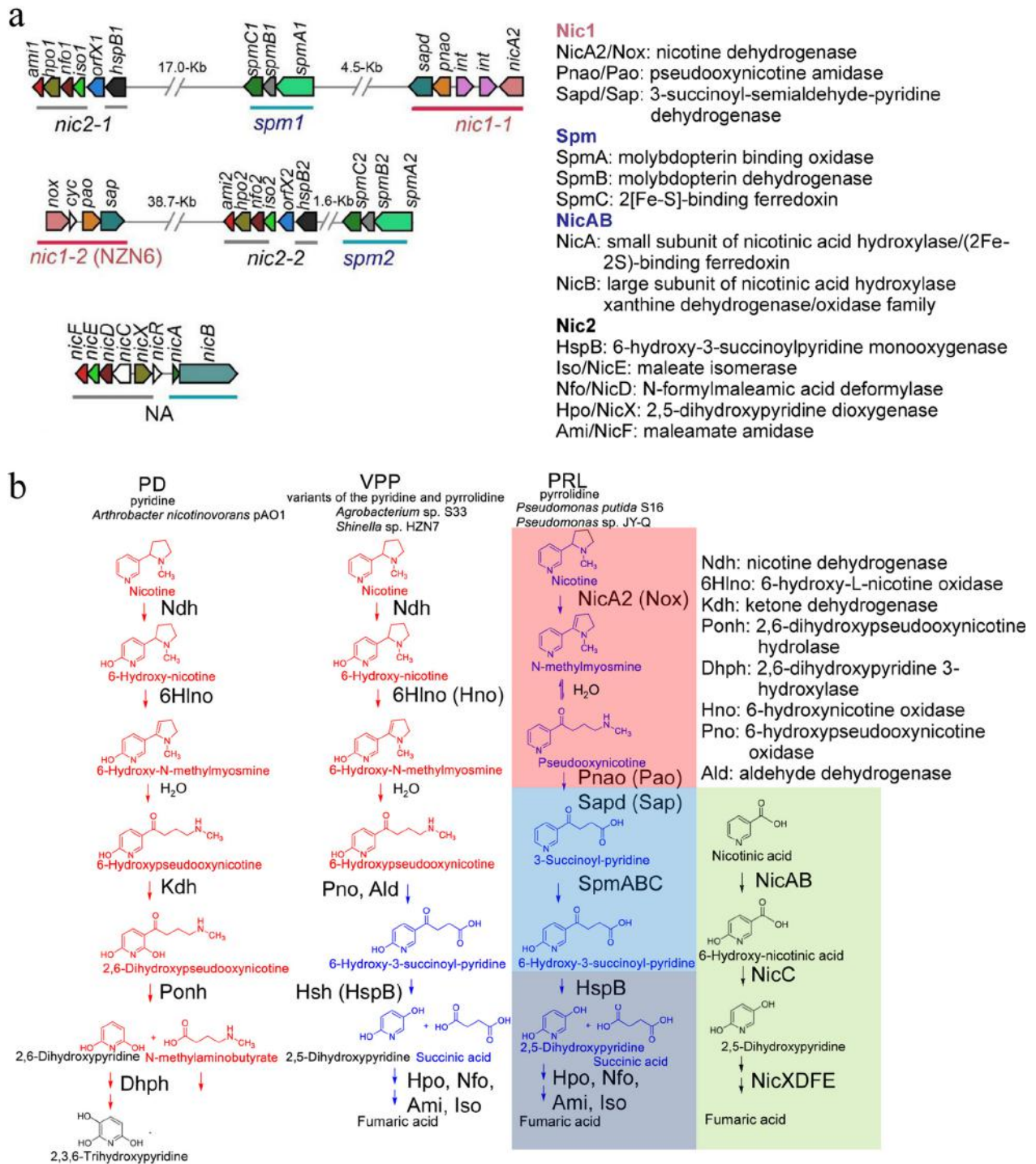
Three nicotine degradation pathways have been determined in bacteria: the pyridine (1, 2) and pyrrolidine pathways (3, 4) and their hybridized variant (VPP pathway) (5, 6). The pyrrolidine pathway has been widely shown in the *Pseudomonas* species (7–9) and consists of three independent functional modules, Nic1, Spm, and Nic2, representing the up-, mid-, and downstream portions of the pyrrolidine pathway, respectively. The *nic1-1* and *nic1-2* clusters in *Pseudomonas* sp. strain JY-Q contain the genes encoding NicA2/Nox (nicotine dehydrogenase), Pnao/Pao (pseudooxynicotine amine oxidase), and Sapd/Sap (3-succinoylsemialdehyde pyridine dehydrogenase), which constitute the Nic1 module accounting for the transformation of nicotine to 3-succinoyl-pyridine (SP) (10, 11). The Spm module contains the complex enzyme Spm (3-succinoyl-pyridine monooxygenase), which consists of SpmA (molybdopterin-binding oxidase), SpmB (molybdopterin dehydrogenase), and SpmC (2Fe-2S-binding ferredoxin), which account for the conversion of 3-succinoyl-pyridine (SP) to 6-hydroxy-3-succinoyl-pyridine (HSP). The Nic2 module, comprising serial enzymes HspB (6-hydroxy-3-succinoylpyridine monooxygenase), Hpo (2,5-dihydroxypyridine dioxygenase), Nfo (N-formylmaleamic acid deformylase), Ami (maleamate amidase), and Iso (maleate isomerase), conducts energy production via conversion of 6-hydroxy-3-succinoyl-pyridine (HSP) to 2,5-dihydroxypyridine (2,5-DHP) and finally to succinic acid and fumaric acid (12–15) (Fig. 1).

In *Pseudomonas* and *Bordetella* species (16, 17), the nicotinic acid (NA) degradation pathway has been well identified and comprises two functional modules, NicAB and NicXDFE (17, 18). NicAB hydroxylates NA to 6-hydroxy-nicotinic acid (6-HNA) (18). NicC transforms 6-hydroxy-nicotinic acid (6-HNA) to 2,5-dihydroxypyridine (2,5-DHP) by oxidative decarboxylation, and NicXDFE accounts for the transformation process from 2,5-dihydroxypyridine (2,5-DHP) to fumaric acid (17, 19–21). The enzymes in the NicXDFE module might also have an additional role in transforming nicotine-related intermediates because of their sequence and functional similarity to those in the Nic2 module (8, 9). This potential function of the NicXDFE module was verified in our previous study, which showed that the JY-Q mutant with a dual deletion of *Spm1* and *Spm2* genes in the Nic2 module could also grow on basic salt medium (BSM) containing nicotine (3). Our previous study reported that the nicotine and NA degradation pathways coexist in a single strain, based on our comparative genomics analysis of JY-Q (3).

Interestingly, JY-Q possesses two sets of homologous gene clusters corresponding to each of the three modules, Nic1, Spm, and Nic2 (3, 12, 13, 22). The JY-Q mutants with dual deletion of nicotine dehydrogenase genes (*nicA2* and *nox*) in the Nic1 module lose the ability to grow on BSM containing nicotine (3). However, the mutant with dual deletion of the homologous genes (*spm1* and *spm2*) in the Spm module still grows on BSM containing nicotine (Fig. 2). This result strongly suggests that there is an alternative pathway, instead of Spm, that is responsible for SP catabolism in JY-Q.

In addition, the contribution of other auxiliary factors or regulatory elements, such as SirA2 (sulfur transferase) and MoaE (molybdopterin synthetase), to SP transformation in JY-Q needs to be evaluated. SirA2 in *Pseudomonas* sp. strain HZN6 is essential for reduction of SP to HSP (22, 23), which is ubiquitous in bacteria and is fundamental for primary metabolism and cell viability (23–25). MoaE in *Pseudomonas putida* S16 is crucial for molybdopterin cytosine dinucleotide (MCD) biosynthesis, and MCD, rather than molybdopterin guanine dinucleotide (MGD), is the cofactor of Spm (22, 26, 27).

In this study, we investigate the functionality of two Spm enzymes and compare their contributions to nicotine degradation in *Pseudomonas* sp. JY-Q. A further aim is to investigate and determine any potential alternative pathway for SP transformation in the *spm* deletion mutant of JY-Q. We also attempt to illustrate the genetic and regulatory mechanisms, such as high nicotine tolerance and nicotine degradation ability, in *Pseudomonas* sp. JY-Q and to facilitate further improvements of bacterial nicotine degradation.



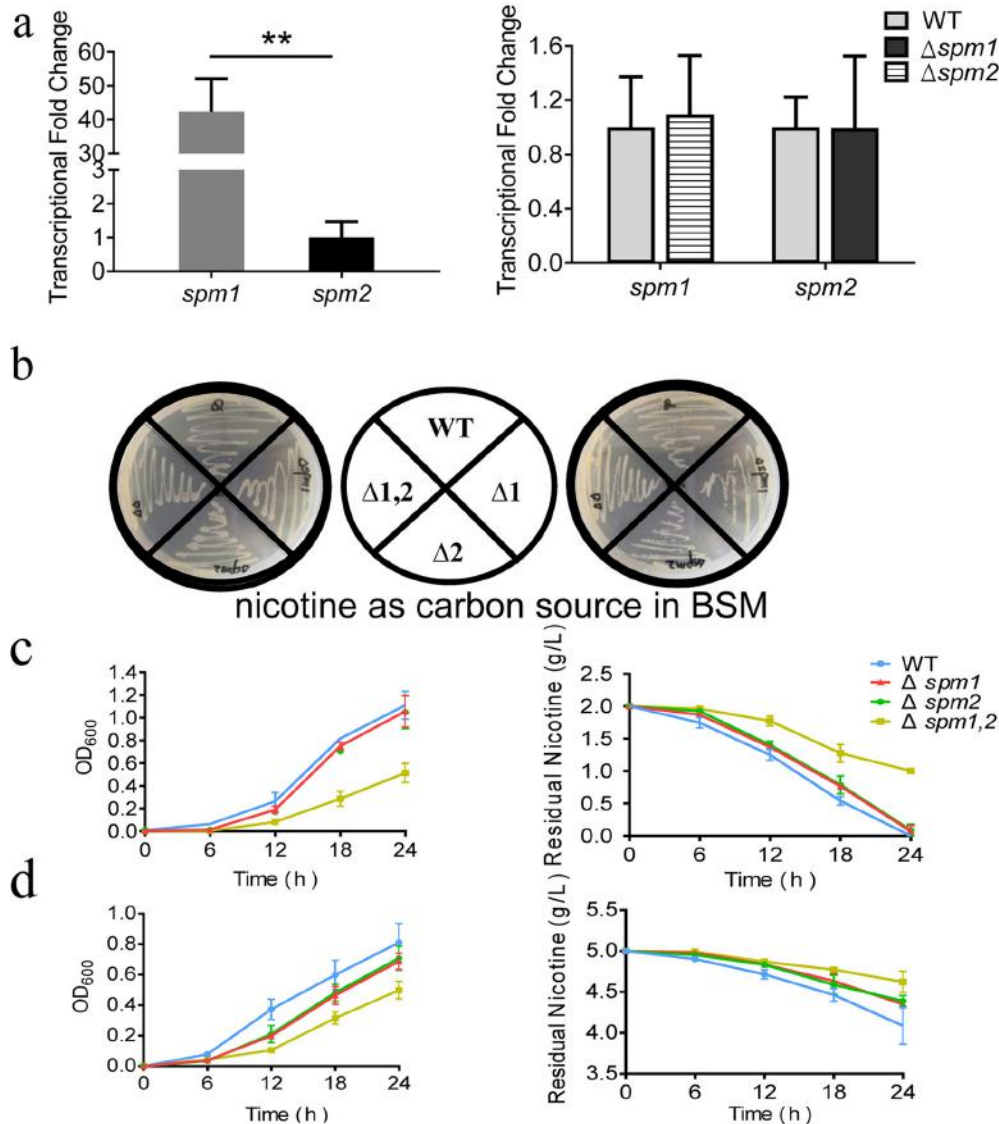


FIG 2 Growth and nicotine degradation profiles of strain JY-Q and related $\Delta spm1$ and/or $\Delta spm2$ deletion mutants. (a) Transcription difference between two homologous *spm* genes in the wild type (WT) with 2 g/liter nicotine as the sole carbon/nitrogen source (left); transcription difference of *spm* between WT and the mutant with another *spm* knockout with 2 g/liter nicotine as sole carbon/nitrogen source (right). (b) Growth difference between the WT and *spm* mutants on BSM agar plate with 2 g/liter (left) or 5 g/liter (right) nicotine. (c) Growth and nicotine degradation curves of the WT and mutants in liquid BSM with 2 g/liter nicotine. (d) Growth and nicotine degradation curves of the WT and mutants in liquid BSM with 5 g/liter nicotine.

RESULTS

Spm1 and Spm2 both contribute to SP conversion in strain JY-Q. The expression of *spm1* and *spm2* was analyzed via reverse transcription-quantitative PCR (RT-qPCR) analysis to evaluate potential different contributions of homologous genes in the Spm module. The results showed that the transcription level of *spm1* in the JY-Q strain was significantly higher than that of *spm2* when nicotine was added as the sole carbon/nitrogen source in BSM (Fig. 2a). However, when *spm1* was knocked out, the resultant $\Delta spm1$ mutant did not exhibit an increase in the transcription level of *spm2*, nor did *spm2* knockout increase the transcription level of *spm1* (Fig. 2a). Furthermore, the nicotine degradation abilities of the mutants with single and dual *spm* disruptions were examined. No significant growth differences between the wild type (WT) and the mutant

strains were detected on a BSM plate containing nicotine (Fig. 2b). However, in liquid BSM with 2 g/liter and 5 g/liter nicotine, the mutant strains exhibited decreases in both the cell growth rate and the nicotine degradation rate (Fig. 2c and d). Effects were more obvious in liquid BSM with 5 g/liter nicotine. Among all the mutant strains, the *spm1 spm2* dual disruption strain showed significant decreases in both the cell growth rate and the nicotine degradation rate. Thus, there is no significant difference in the contributions of two homologous *spm* genes to nicotine degradation, and an additive effect might be rendered by homologous genes of the Spm module.

Moreover, the mutant with a double *spm* knockout could still grow and degrade nicotine. This result is different from that observed for *P. putida* strain S16, whose Δspm mutant could not grow and no nicotine removal was observed when it was cultured in minimal salt medium (MSM) supplemented with nicotine (4). Thus, there might be an alternative pathway in strain JY-Q, rather than Spm, that transforms SP.

SirA2 is essential in JY-Q, but not only for SP transformation. SirA2 has been reported to participate in SP conversion by *Pseudomonas* sp. strain HZN6, because the mutant of HZN6 with a *sirA2* deletion ($\Delta sirA2$ mutant) lost the ability to grow on MSM containing nicotine (21). Based on comparative genomics analysis, the SirA2 in JY-Q is 98% identical to that in *P. putida* S16 (28) and 76% identical to that in strain HZN6 (23). Transcription levels in the wild type and in $\Delta spm1$ or $\Delta spm2$ mutants were measured to investigate whether SirA2, instead of Spm, could transform SP. The results showed that transcription levels of *sirA2* in $\Delta spm1$ or $\Delta spm2$ mutants were both significantly lower than that in the wild type, and its expression in the wild type was not induced by nicotine (Fig. 3a and b). However, *sirA2* transcriptional levels in the $\Delta spm1 \Delta spm2$ strain are nearly identical to that in the WT grown in BSM plus 2 g/liter nicotine. This finding showed an increase of the *sirA2* transcriptional level in the $\Delta spm1 \Delta spm2$ isolate compared to that in $\Delta spm1$ and $\Delta spm2$ mutants. The mutant strain with an *sirA2* knockout ($\Delta sirA2$ mutant) grew on Luria-Bertani (LB) medium. However, it lost its ability to grow not only on BSM containing nicotine but also on BSM containing glucose or glycerol as the only carbon source and including $(NH_4)_2SO_4$ as a nitrogen source (Fig. 3c). This result suggested that SirA2 in strain JY-Q might play a role in the metabolism of a variety of nutritional substances and that it also plays a nonexclusive role as the sulfur transferase in SP metabolism, similar to that in *Pseudomonas* sp. strains HZN6 and S16 or *Escherichia coli* BL21. In addition, multiple-sequence alignment for the above-described SirA2 homologs also showed their similarity (Fig. 3d). SirA has been verified as a sulfur transferase in *E. coli*. Thus, we inferred that SirA2 could be a sulfur transferase and also be an important component that was related to JY-Q growth on BSM plus nicotine but indirectly participated in nicotine metabolism. Thus, SirA2 in strain JY-Q might be an auxiliary factor or regulatory element to facilitate SP transformation in nicotine degradation, rather than an alternative SP α -position hydroxylase. In conclusion, SirA2 is certainly not a substitute for Spm in JY-Q.

Identification of the role of JY-Q_NicAB in nicotine degradation. After we excluded SirA2, other possible isozymes were mined using self-customized comparative genomics analysis (29, 30) and by protein family identification (31, 32). Using the following criteria, we acquired the likely candidates, namely, (i) subunits coding for homology domains of SpmABC including 2[Fe-S] as the electron carrier and (ii) a molybdenum-containing hydroxylase. Finally, two possible isoenzymes, the aldehyde dehydrogenases Ald1 (gene locus tag *AA098_17805*) and Ald2 (gene locus tag *AA098_16795*) were predicted. The genes corresponding to Ald1 and Ald2 and their neighbors encode significant candidates bearing rearranged domains of SpmABC (28) (Fig. 4a). Interestingly, nicotine dehydrogenase (Ndh_{SML}) from *Paenarthrobacter nicotinovorans* (1) and molybdenum-containing nicotine hydroxylase (VppA) from *Ochrobactrum* sp. strain SJY1 (27), both showing α -position hydroxylation of the pyridine ring, contained these functional domains. A gene extremely similar to *ald2* (*AA098_16795*) was also found in strain S16. However, the *AA098_16795* homolog might not be necessary for SP transformation in S16, since no cell growth was observed when *spm* was deleted (4). Additionally, *ald1* (*AA098_17805*) and its adjacent gene (*AA098_17800*) exhibit high

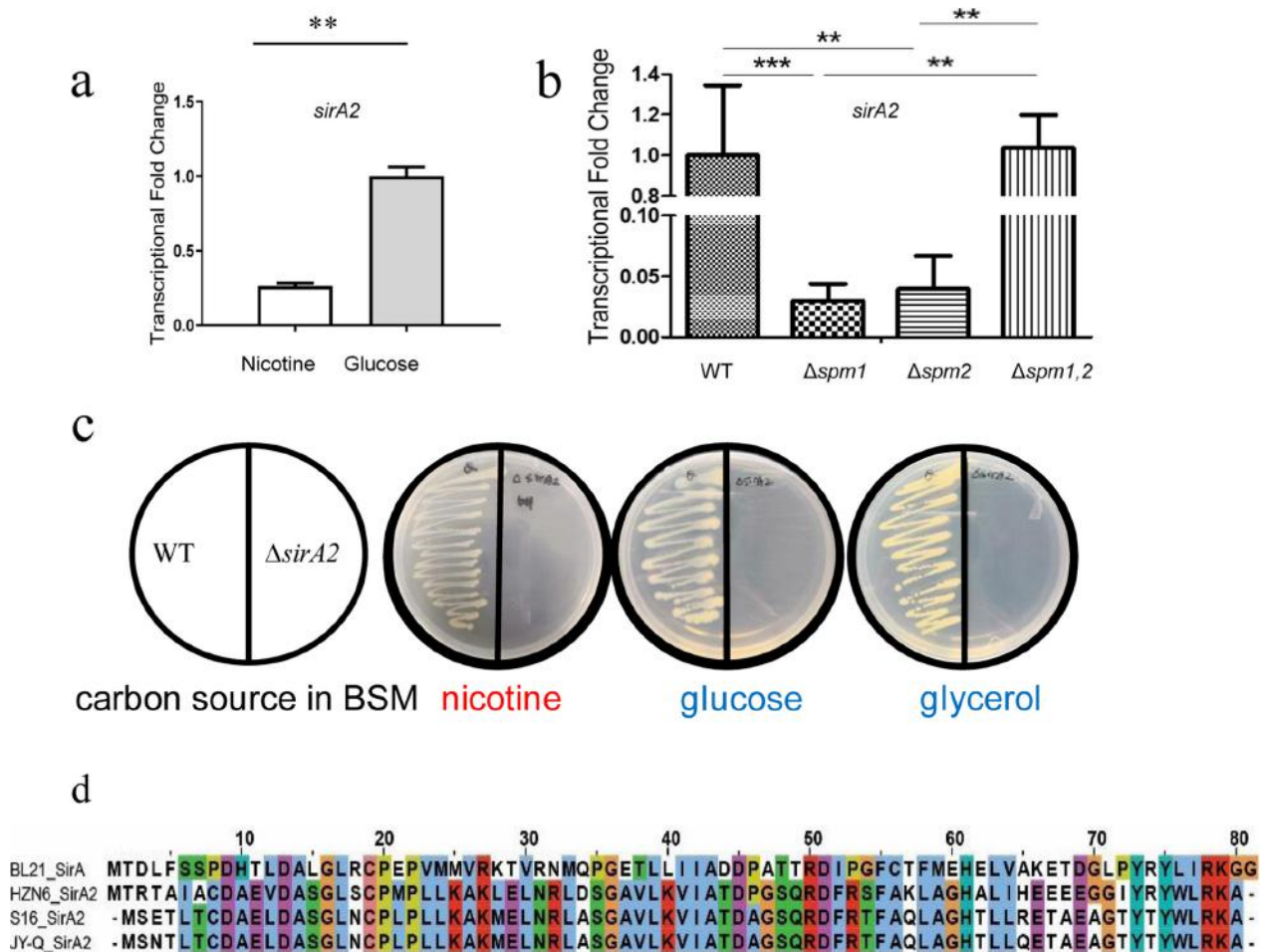


FIG 3 Essentiality examination of *sirA2* for nicotine metabolism. (a) Transcription difference of *sirA2* in the WT (wild type) on BSM supplemented with only nicotine or with glucose and $(\text{NH}_4)_2\text{SO}_4$. (b) *sirA2* transcriptional changes if two Spm modules were deleted individually or together; the WT and *spm* mutants were cultured on BSM with 2 g/liter nicotine. (c) Growth difference between the WT and the $\Delta sirA2$ mutant on BSM plates supplemented with nicotine (left panel), glucose (middle panel), and glycerol (right panel). (d) Comparison of SirA (sulfur transferase) homologues encoded by strains JY-Q, HZN6, S16, and BL21.

sequence similarities to *nicB* and *nicA*, respectively, in the KT2440 strain. NicA and NicB are two components of the enzyme NicAB, which is responsible for NA hydroxylation in strain KT2440 (Fig. 4a). The amino acid sequence of Ald1 in JY-Q is 98.15% identical to that of NicB (Fig. 4b), while 2[Fe-S] subunits in JY-Q are almost the same as NicA in KT2440. Additionally, the rearranged molybdenum cofactor (Mo-Co) binding motifs (organization 2-1-3) of NicAB were also similar to SpmA (motif organization 1-2-3). In conclusion, Ald1 should be annotated as NicB (Ald1 corresponding to NicB in JY-Q) as one component of the enzyme NicAB in JY-Q.

In addition, the similarity in structure of the substrates recognized between NA and SP suggested an additional function for JY-Q_NicAB in SP transformation. We examined the response of *ald1* (*nicB*) and *ald2* in wild-type JY-Q to the addition of nicotine in BSM. The transcriptional level of *ald1* (*nicB*) was upregulated to a higher level than that of *ald2* in the presence of nicotine (Fig. 5a). Interestingly, when two homologous genes, *spm1* and *spm2*, were knocked out, the $\Delta spm1 \Delta spm2$ mutant strain exhibited an increase in *ald1* and *ald2* transcript levels, indicating a potential complementary function of Ald1 for the Spm module (Fig. 5b). Subsequently, when the genes were deleted, the resultant $\Delta ald1$ ($\Delta nicB$) mutant strain exhibited a significant decrease of cell growth in BSM supplemented with nicotine as the sole carbon source, while the $\Delta ald2$ mutant

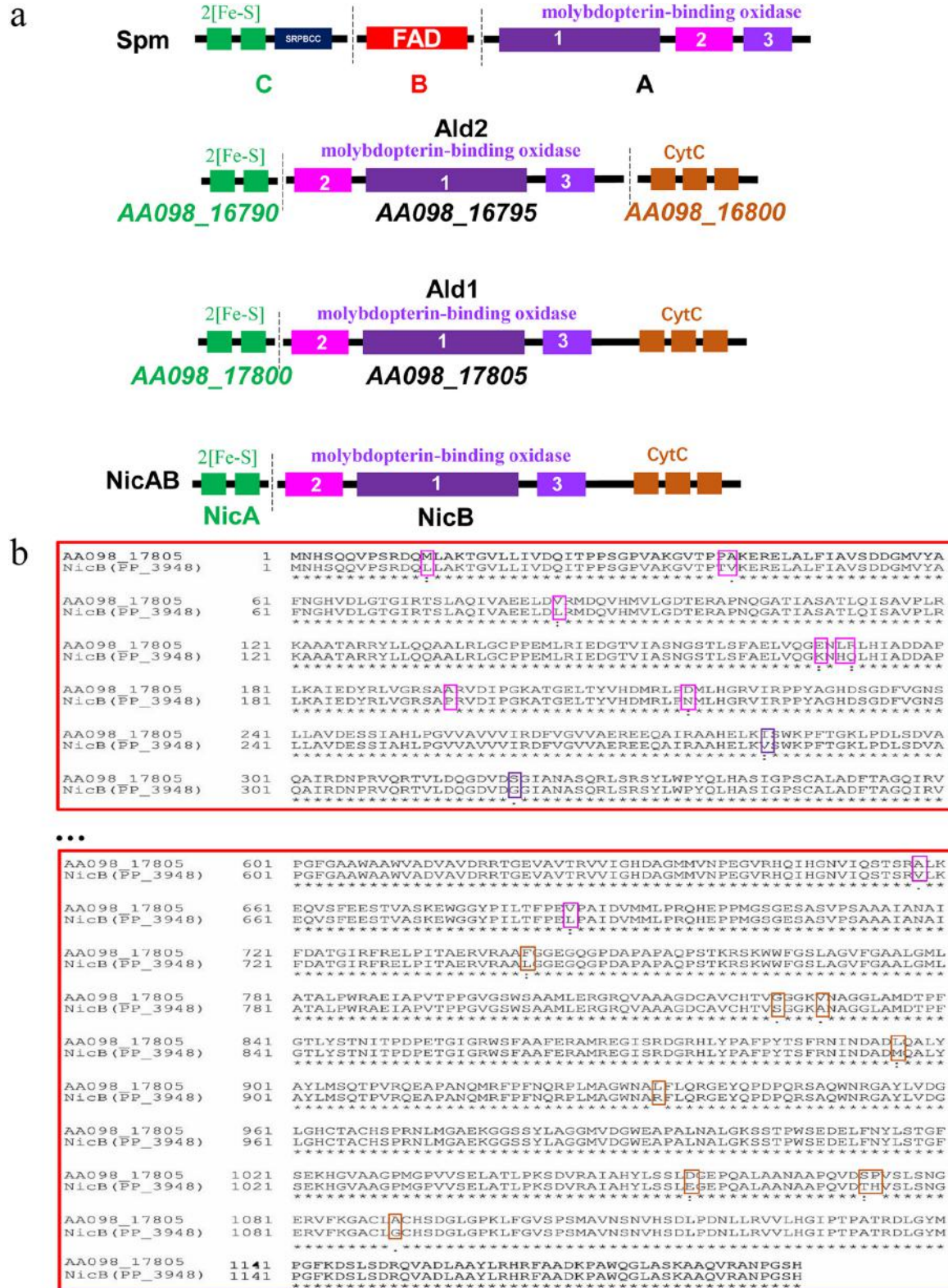


FIG 4 Comparative analysis for Spm and two Ald-like alternative candidates. (a) The Spm module is comprised of three enzyme components, respectively named A, B, and C. 2[Fe-S], as the electron recipient, and one molybdopterin-binding oxidase consisting of three motifs were both (Continued on next page)

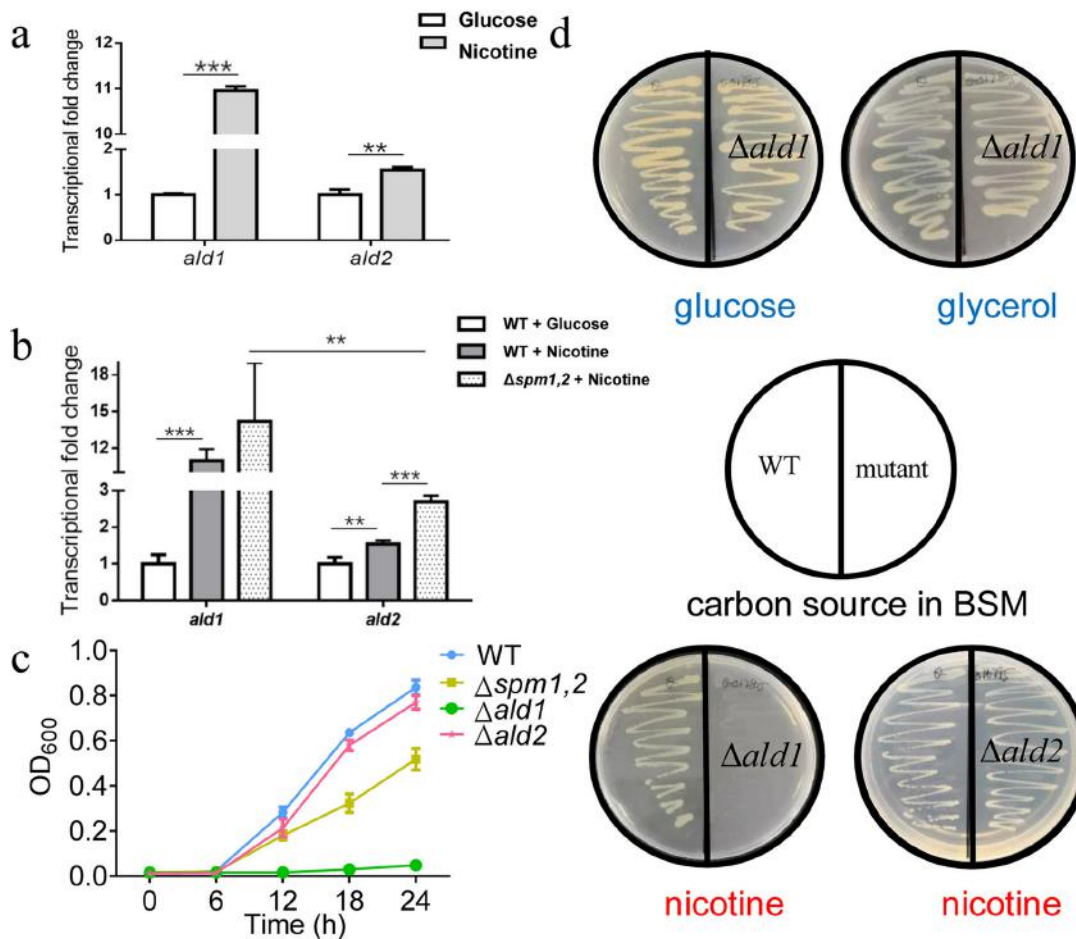


FIG 5 Examination of JY-Q_NicAB (Ald1) essentiality for nicotine metabolism. (a) Transcription difference of *ald1* and *ald2* in the WT on BSM supplemented with nicotine as the sole carbon/nitrogen source or with glucose and $(NH_4)_2SO_4$. (b) Transcriptional changes of *ald1* and *ald2* if *spm1* and *spm2* are deleted; the WT and *spm* mutants were cultured in BSM plus 2 g/liter nicotine. (c) Growth curves of wild-type JY-Q and its mutants in BSM with 2 g/liter nicotine. (d) Growth difference between the WT and $\Delta ald1$ (upper) on BSM plates with glucose (left) and glycerol (right); growth difference among the WT and $\Delta ald1$ or $\Delta ald2$ mutants (lower) on BSM supplemented with nicotine.

strain did not (Fig. 5c and d). However, the $\Delta ald1$ ($\Delta nicB$) JY-Q strain could be cultured in BSM supplemented with glucose and glycerol (Fig. 5d). This is different from the $\Delta sirA2$ strain, which lost cell growth not only on nicotine but also on glycerol and glucose (Fig. 3c).

The above results largely present the essentiality of *nicB* in the JY-Q strain for nicotine-related intermediate metabolism. Nevertheless, the copresence of nicotine and NA degradation genes is meaningfully associated with highly efficient nicotine metabolism in JY-Q. In conclusion, the whole NA degradation gene cluster, including *nicAB* and *nicXDFE*, could be involved in nicotine metabolism for the JY-Q mutant with *spm1* and *spm2* deleted. This leads to a conclusion different from the report that the NA degrada-

FIG 4 Legend (Continued)

characterized for Ald1 and Ald2. The arrangement of these three motifs (indicated by 1, 2, and 3) is different between Spm and Ald. In addition, three CytC motifs were found in Ald1. The similar CytC domain was encoded by the gene adjacent to *ald2*. Both SpmABC and Ald2 homologs were observed in the genomes of strains S16 and JY-Q. Ald1 was only found in strain JY-Q. FAD, FAD binding; SRPBCC, SRPBCC ligand binding. (b) Multiple-sequence alignment for two NicB proteins retrieved respectively from strains JY-Q and KT2440. Amino acid residual variants in different motifs are denoted by rectangles. Moreover, absolutely identically and relatively (similar properties) conserved amino acid sites are indicated by additional asterisk (*) and colon (:) symbols, respectively.

tion-related gene cluster carried by strain KT2440 could not confer nicotine removal capability (16).

Expansion of JY-Q_NicAB substrate from NA to SP in strain JY-Q. The NicAB function of transforming NA into 6-HNA has been verified in *Pseudomonas* species. One might ask if it really has the function of transforming SP into HSP. A large quantity of purified wild or recombinant NicAB enzyme is required to test this hypothesis. However, Spm and NicAB are both molybdopterin cytosine dinucleotide (MCD)-dependent enzymes. MCD can be produced in *Pseudomonas* and *Arthrobacter* species (31–33), while *Escherichia coli* can only synthesize Mo-Co MGD (molybdopterin guanine dinucleotide) (33). Thus, *E. coli* failed to express functional Spm (4). In this study, *P. putida* S-1, isolated by our group from activated sludge, was chosen as the expression host because of its inability to degrade NA (34, 35).

Next, *ald1* plus *AA098_17800* (as a whole, *JY-Q_nicAB*) and *ald2* plus *AA098_16790* (coding for 2[Fe-S]) were introduced into *Pseudomonas putida* S-1 using the pBBR1MCS5 vehicle. The resultant recombinant strains, S-1/pBBR-*nicAB* and S-1/pBBR-*ald2-2*[Fe-S], exhibited white and yellow tints when suspended in liquid culture, respectively, while the wild-type S-1 and S-1/pBBR vehicle strains both exhibited a pink color (Fig. 6a). Subsequently, whole-cell proteins were harvested, and SDS-PAGE was conducted to verify *nicAB* expression. The protein of the band highlighted with a red rectangle in Fig. 6b might be NicAB, of which the theoretical molecular weight is 127.7 kDa.

In strain S-1/pBBR-*nicAB*, SP might be transformed by JY-Q_NicAB and result in the accumulation of the theoretical product, HSP, because this strain lacks other genes for NA degradation. Thus, a reaction mixture was prepared, using resting cells with S-1/pBBR-*nicAB* and SP with a final concentration of 1.0 mg/ml, to test the function of JY-Q_NicAB. SP removal and HSP production were examined by liquid chromatography-mass spectrometry (LC-MS). Both SP (molecular ion at m/z 178.17 [M-H]⁻ and fragment ion at 134.17 [M-H]⁻; Fig. 7a) and HSP (molecular ion at m/z 194.17 [M-H]⁻ and fragment ion at 150.17 [M-H]; Fig. 7b) were identified in the reaction mixture. The JY-Q_NicAB expressed in strain S-1 could transform SP to HSP (Fig. 7c). However, HSP could not be observed in the LC-MS spectra for strain S-1/pBBR-*ald2-2*[Fe-S]. In conclusion, JY-Q_NicAB exhibited a role in SP transformation (Fig. 7d).

However, it is still necessary to test the function of JY-Q_NicAB for NA transformation into 6-hydroxynicotinic acid (6-HNA), which is the function of NicAB in strain KT2440 (16, 18). Thus, resting cells of S-1/pBBR-*nicAB* were prepared and mixed with NA at a final concentration of 1.0 mg/ml in a reaction mixture. NA removal and 6-HNA production were both detected by LC-MS (Fig. 7e and f). This result indicated that JY-Q_NicAB could oxidize NA to 6-HNA.

Taken together, these results indicate that JY-Q_NicAB is a hydroxylase that could oxidize SP and NA to HSP and 6-HNA, respectively. In other words, JY-Q_NicAB exhibited an additional role for the transformation of succinoyl-pyridine.

Interestingly, SpmABC is the exclusive determinant accounting for the conversion of SP into HSP in some nicotine-degrading strains, such as S16 (4), while SpmABC in JY-Q is not the exclusive determinant accounting for the conversion of SP into HSP, and JY-Q_NicAB performs a more effective role in transforming SP than the two Spm modules. In other words, the NA degradation pathway in JY-Q, as a whole, can be regarded as an alternative/synergistic pathway for nicotine metabolism, in which sequential NicXDFE might nonexclusively metabolize nicotine-related intermediates for energy production. In addition, this newly found additional role of NicAB in strain JY-Q provides a flexible salvage mechanism for the strain, if Spm is impaired, to coordinate fitness demand and energy production.

DISCUSSION

In the past few decades, three nicotine degradation pathways have been determined in bacteria (4, 36, 37). Most strains of *Pseudomonas* were found to utilize the

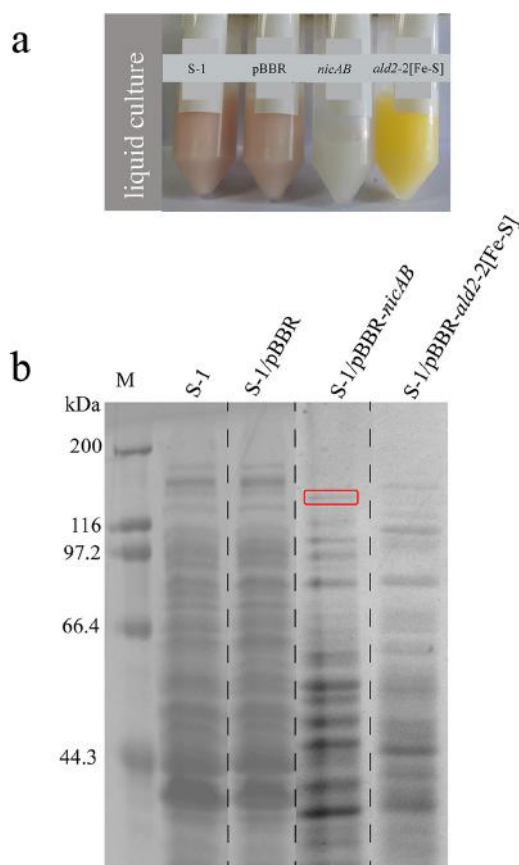


FIG 6 Heterologous expression and SDS-PAGE examination of Ald-like proteins. (a) Tint changes for liquid culture suspension of strain S-1 after *ald1* and *ald2* introduction. (b) SDS-PAGE of harvested whole-cell proteins. S-1-expressed Ald1 is indicated by the red rectangle.

pyrrolidine pathway (7–9), whose regulatory molecular mechanisms have been illustrated in several publications (7, 14, 25, 38). The nicotine-degrading strain *Pseudomonas* sp. JY-Q was isolated from tobacco waste aqueous extract (TWE), which contains high concentrations of nicotine (above 15 g/liter) and glucose (150 g/liter) and is at a low pH (~4). This strain is tolerant and shows the ability to degrade a high content of nicotine, possibly through a special mechanism that has prompted our investigation.

The remarkable finding is that there are two duplicated homologous gene clusters for each of the up-, mid-, and downstream portions (namely, functional modules Nic1, Spm, and Nic2) of the pyrrolidine pathway in JY-Q (3, 8). Although multiple copies of some catabolism-related genes are common in eukaryotes, less is known about prokaryotes (29, 36, 37, 39, 40). Recently, there have been a few academic reports of duplicated genes contributing to pollutant catabolism, such as two homologous but not identical nicotine-degrading gene clusters found in JY-Q (8) and the cooccurrence of two dibutyl phthalate-degrading clusters in plasmid pQL1 of *Arthrobacter* sp. strain ZJUTW (41).

It has also been shown that duplicated homologous gene clusters (or genes) exhibit additive or synergistic effects in JY-Q. However, the homologous genes (clusters) in duplicate Nic1, Spm, and Nic2 modules exhibit different levels of effectiveness that might result from their sequence variants. This finding also highlights a new strategy to improve nicotine degradation by introducing adaptability-related determinants and

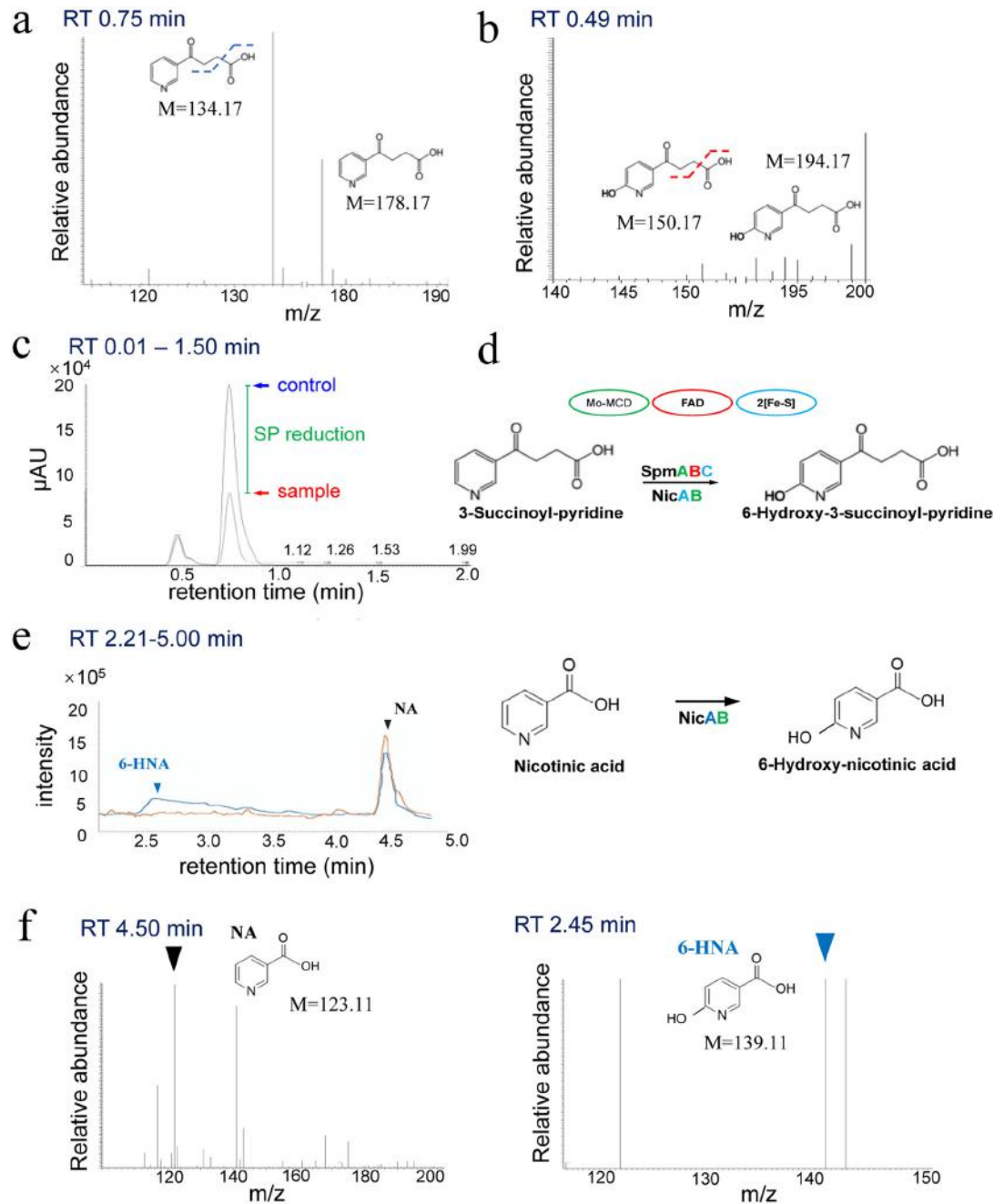


FIG 7 JY-Q_NicAB could perform an alternative role in transforming SP into HSP. (a) SP standard chemicals identified by mass spectrum (MS) technologies. (b) MS-detected HSP resulting from SP hydroxylation mediated by S-1/pBBR-*nicAB*. (c) SP elimination by S-1/pBBR-*nicAB* (48-h sampling, indicated by red) compared to two controls (0-h sampling of S-1/pBBR-*nicAB* and S-1/pBBR, indicated by blue), of which the absorption peak was examined by high-performance liquid chromatography (HPLC). (d) Proposed working model of SP transformation to HSP by SpmABC and JY-Q_NicAB for SP utilization, and model of NA transformation to 6-HNA by JY-Q_NicAB. The similar subunits of SpmABC and NicAB were indicated by matching colors. Mo-MCD, sulfurated molybdopterin cytosine dinucleotide cofactor. *E. coli* uses molybdopterin guanine dinucleotide (MGD) instead of MCD as the Mo-Co. FAD, FAD binding domain; 2[Fe-S], iron-sulfur cluster. JY-Q_NicAB could transform NA into 6-HNA as well. (e) NA reduction and 6-HNA yield indicated functionality of JY-Q_NicAB as a nicotinic acid hydroxylase. Red, control group; blue, treatment with S-1/pBBR-*nicAB*. (f) NA (black) and 6-HNA (blue) spectra of LC-MS detected in the reaction mixture of NA and S-1/pBBR-*nicAB* resting cells.

additional inducers/synergists into both homologous gene clusters, mimicking the numerous successes described in previous publications (26, 42).

In our previous study, we illuminated two phenomena of interest, namely, (i) NA degradation-related NicX (a homolog of Hpo belonging to Nic2) contributed to JY-Q growth with nicotine, and (ii) in-frame deletion of two Spm resulted in a significant decrease in, but not a loss of, the ability to degrade nicotine. There may be a diversified alternative strategy instead of the function of Spm.

First, we attempted to survey the substitute pathway for Spm through gene or protein sequence similarity identification. SirA2 reportedly participates in the SP conversion by strain HZN6, and SirA2 in JY-Q is 76% identical to that in strain HZN6 (23). The $\Delta sirA2$ mutant strain of JY-Q lost the ability to grow on BSM plus nicotine, similarly to HZN6 (23). However, it lost the ability to grow not only on BSM plus nicotine but also on BSM containing glucose or glycerol as the only carbon source and with $(NH_4)_2SO_4$ as the sole nitrogen source (Fig. 3c). SirA2 in strain JY-Q or in HZN6 might play a role as the sulfur transferase in SP metabolism. SirA2 was indirectly related to bacterial growth in this study and might be an auxiliary factor or regulatory element facilitating SP transformation by α -position hydroxylation. In conclusion, SirA2 is certainly not a substitute for Spm in JY-Q.

As a determinant of NA degradation in KT2440 (16), the NicB homolog showed a low similarity (24% identity at the protein sequence scale) to SpmA in JY-Q. However, the rearrangement architecture of NicAB subunits suggests its functional similarity to SpmABC in JY-Q (Fig. 4a). Possible cooperation of SpmABC and NicAB for JY-Q may allow the utilization of nicotine. In addition, the NA degradation pathway consists of two functional modules, NicAB and NicXDFE. NicAB can oxidize NA but not nicotine. NicC seems not to be related to nicotine metabolism, because no homolog of NicC (6-HNA monooxygenase) is found among nicotine catabolism enzymes, based on sequence similarity analysis. NicXDFE can mediate 2,5-DHP conversion to fumaric acids (16), whose function is highly similar to that of module Nic2 (5, 6).

In this study, when *nicAB* (*ald1-2*[Fe-S]) in JY-Q was deleted, the mutant did not grow on BSM supplemented with nicotine as the sole carbon and nitrogen source but could grow well on BSM supplemented with glucose or glycerol plus $(NH_4)_2SO_4$ (Fig. 5c and d). These findings sufficiently illustrated the indispensable role of JY-Q *nicAB* in nicotine-related metabolism. VppA (27), Spm (4), and NicAB (16) can account for α -position hydroxylation of the pyridine loop in VPP/pyrrolidine-related nicotine metabolism and NA degradation. However, strain KT2440 carrying an *nicAB* prototype could not grow in minimal salt medium (MSM) supplemented with SP (23). NicB in JY-Q is not completely the same (98.15% identity, 1,165/1,187 matching amino acids) as NicB in KT2440 (18, 19), and the variability of 22 amino acid sites might contribute to the changes in the compactness and flexibility of NicAB in JY-Q, making it able to accommodate the binding and reaction of SP, whose chemical structure is similar to that of NA. However, the possible effect of architectural rearrangement of subunits in NicB on enzyme function change will require further studies to clarify.

As shown in Fig. 4, NicAB consists of two components, (i) NicA (2[Fe-S]) for electron recipient/transport and (ii) NicB (Ald1), a hydroxylase-like protein containing a redox site formed by cofactor molybdopterin cytosine dinucleotide (MCD) and three CytC (conserved cytochrome c) domains. Ald1 was found to encode the same domains but with rearranged subunits compared to SpmABC. However, its architecture is identical to the NicAB progenitor in KT2440. This sequence analysis also underlined the possibility of reorganization for the electron donor/recipient chain. Therefore, *E. coli* is an inappropriate host cell to perform the NicAB function, because it cannot synthesize this particular cofactor, MCD (26), to bind and thereby activate NicAB (33). In this study, we thus selected another strain, *P. putida* S-1, to express *nicAB*, because S-1 is phylogenetically close to JY-Q but not able to metabolize NA. When *nicAB* was transferred into the wild-type strain S-1, which is not capable of SP hydroxylation (verified by sequential LC-MS assay for strain S-1 cultured with SP as the sole carbon and nitrogen source), the resultant S-1/pBBR-*nicAB* strain exhibited the ability to oxidize SP (Fig. 7), suggesting that

Ald1 in JY-Q (with high identity to NicB in KT2440) has an expanded function for transformation of SP to HSP. Furthermore, Ald2 was found to be only 30% identical to, but to have similar domain organization as, Ald1. No HSP production was observed for strain S-1 bearing *ald2-2*[Fe-S]. This finding suggests that this difference might result from Ald1 C-terminal extended CytC as the electron carrier and a number of variants for amino acid residues between Ald1 and Ald2.

In short, the enzymes of the NA degradation pathway have an additional role in catalyzing nicotine-related chemicals, such as SP and 2,5-DHP, instead of the enzymes in modules Spm and Nic2. This finding provides a novel insight into the association between nicotine and NA degradation pathways. In strain JY-Q, the NA degradation pathway seems able to assist the pyrrolidine pathway of nicotine degradation if its Spm module is interrupted. It is also feasible that two homologous nicotine degradation gene clusters (*nic1-spm-nic2*) and one NA degradation gene cluster (*nicABCXDFE*) in the JY-Q genome cooperate together for its adaptability in encountering the stress of high nicotine concentrations in tobacco waste extract.

MATERIALS AND METHODS

Chemicals and media. Nicotine (99% purity) was purchased from Fluka Chemie GmbH (Buchs, Switzerland), and related enzymes for DNA manipulation were purchased from TaKaRa Biotechnology Co., Ltd. (Dalian, China). 3-Succinoyl-pyridine (SP) was purchased from Toronto Research Chemicals Inc. (North York, ON, Canada). All other reagents and solvents were of analytical or chromatographic grade and commercially available.

Luria-Bertani (LB) medium, basic salt medium (BSM), and phosphate-buffered saline (PBS) were used in this study. Each liter of LB medium contained yeast extract, 5.00 g; tryptone, 10.00 g; and NaCl, 10.00 g in 1 liter of double-distilled water (ddH₂O). Each liter of BSM comprised Na₂HPO₄, 5.57 g; KH₂PO₄, 2.44 g; K₂SO₄, 1.00 g; MgCl₂·6H₂O, 0.20 g; MnCl₂·4H₂O, 0.40 mg; CaCl₂, 1.00 mg; and FeCl₃·6H₂O, 1.00 mg, with ddH₂O added up to 1 liter. Nicotine (2.00 or 5.00 g/liter), 10.0 g/liter glycerol, or 4.0 g/liter glucose coupled with 1.00 g/liter (NH₄)₂SO₄ was used as the sole carbon and nitrogen source; they were prepared as BSM plus carbon/nitrogen nutrient medium. PBS (1 liter, pH 7.4) was prepared as follows: NaCl, 8.00 g; KCl, 0.20 g; Na₂HPO₄·12H₂O, 3.58 g; and KH₂PO₄, 0.27 g, dissolved in 1 liter of ddH₂O.

Strains, plasmids, and growth conditions. Strains and plasmids used in this study are listed in Table 1. *Escherichia coli* strains were grown in LB medium at 37°C. *Pseudomonas* strains were grown at 30°C in LB or BSM with different carbon/nitrogen sources. *Pseudomonas* sp. JY-Q was previously isolated from tobacco waste extract (TWE) and is capable of nicotine degradation. Notably, strain JY-Q has been deposited in the China Center for Type Culture Collection (CCTCC no. M2013236), and its genome has been archived in GenBank under accession number CP011525 (8). *Pseudomonas putida* S-1 was isolated from activated sludge and is capable of malodorous 1-propanethiol degradation (34). *E. coli* WM3064 was involved in gene deletion and is the auxotroph for 2,6-diaminopimelic acid (2,6-DAP). It is of note that 0.3 mM 2,6-DAP is essential for further DNA manipulation of strain WM3064 (3). In addition, kanamycin (50 μg/ml) and gentamicin (15 μg/ml) were added for transformant acquisition. Shaking at 180 rpm was used for culturing if not otherwise specified (43).

RNA extraction and RT-qPCR. Gene transcriptional changes in *Pseudomonas* sp. JY-Q and its mutants were compared in the presence or absence of nicotine. Total RNA was retrieved by using RNA Isolator (Vazyme Biotech Co., Ltd., Nanjing), and the HiScriptII Q RT SuperMix qPCR kit (purchased from Vazyme Biotech Co.) was used for reverse transcription. RT-qPCR analysis was performed using the CFX96 real-time PCR detection system (Bio-Rad, Hercules, CA) with ChamQ SYBR qPCR mastermix (TaKaRa). The PCR program was customized as follows: 2 min for predenaturation at 95°C, followed by 40 cycles of 20 s for denaturation at 95°C, 20 s for primer annealing at 60°C, and 20 s for elongation at 72°C. The transcriptional level of 16S rRNA was set as an internal reference. Primers used for RT-qPCR are summarized in Table 2.

Gene manipulation. DNA fragments were cloned from *Pseudomonas* sp. JY-Q by PCR. UF/UR and DF/DR primers were designed to amplify up- and downstream fragments, respectively, for gene knockout, and F/R primers were assigned for heterologous expression (Table 2). DNA fragments, the suicide plasmid pK18mobsacB, and plasmid pBBR1MCS5 were digested with two restriction enzymes and ligated *in vitro*. The ligation products were then transferred into *E. coli* DH5α competent cells, and transformant screening was conducted by appropriate antibiotic together with PCR verification. In this study, we used a double-crossover homologous recombination method to construct knockout mutants. The fidelity of recombination derivatives was selected with appropriate concentrations of kanamycin and 15% sucrose, together with PCR and sequencing verification.

For gene expression, pBBR1MCS5-*ald1* or -*ald2* was transferred into *P. putida* S-1 competent cells to constitute the corresponding heterologous expression derivative by preparing electrocompetent cells. Electroporation was performed at 200 Ω, 2,700 V, and 25 μF using the Gene Pulser Xcell (Bio-Rad Laboratory, Hercules, CA).

Protein ectopic expression and SDS-PAGE detection. *Pseudomonas putida* S-1 and its derivatives were grown at 30°C to an optical density at 600 nm (OD₆₀₀) of ~0.6 and then incubated at 20°C for 16 h.

TABLE 1 Strains and plasmids used in this study

Strain or plasmid	Feature(s) ^a	Source
Strains		
<i>E. coli</i> DH5 α	Host to replicate plasmids	TransGen
<i>E. coli</i> WM3064	Host strain for conjugation; auxotroph	Lab stock
<i>Pseudomonas</i> sp. strain JY-Q	Wild type, able to degrade nicotine	Lab stock
Δ <i>spm1</i>	<i>spm1</i> deleted in JY-Q	This study
Δ <i>spm2</i>	<i>spm2</i> deleted in JY-Q	This study
Δ <i>spm1</i> Δ <i>spm2</i>	<i>spm2</i> deleted from JY-Q Δ <i>spm1</i> strain	This study
Δ <i>sirA2</i>	<i>sirA2</i> deleted in JY-Q	This study
Δ <i>ald1</i> (Δ <i>nicB</i>)	<i>ald1</i> (<i>nicB</i>) deleted in JY-Q	This study
Δ <i>ald2</i>	<i>ald2</i> deleted in JY-Q	This study
<i>Pseudomonas putida</i> S-1	Wild type, unable to degrade NA	Lab stock
S-1/pBBR	pBBR1MCS5 in S-1	This study
S-1/pBBR- <i>nicAB</i>	pBBR1MCS5- <i>nicAB</i> in S-1	This study
S-1/pBBR- <i>ald2</i>	pBBR1MCS5- <i>ald2</i> in S-1	This study
Plasmids		
pK18 <i>mobsacB</i>	Suicide vector, <i>mob</i> ⁺ , <i>sacB</i> , Km ^r	Lab stock
pK18 <i>mobsacB-spm1</i> UD	pK18 <i>mobsacB</i> with up- and downstream fragments of <i>spm1</i>	This study
pK18 <i>mobsacB-spm2</i> UD	pK18 <i>mobsacB</i> with up- and downstream fragments of <i>spm2</i>	This study
pK18 <i>mobsacB-sirA2</i> UD	pK18 <i>mobsacB</i> with up- and downstream fragments of <i>sirA2</i>	This study
pK18 <i>mobsacB-ald1</i> UD	pK18 <i>mobsacB</i> with up- and downstream fragments of <i>ald1</i>	This study
pK18 <i>mobsacB-ald2</i> UD	pK18 <i>mobsacB</i> with up- and downstream fragments of <i>ald2</i>	This study
pBBR1MCS5	Expression plasmid, Gm ^r	Lab stock
pBBR1MCS5- <i>nicAB</i>	pBBR1MCS5 containing <i>nicAB</i>	This study
pBBR1MCS5- <i>ald2</i>	pBBR1MCS5 containing <i>ald2</i>	This study

^aKm, kanamycin; Gm, gentamycin; ^r, resistance.

The cells were centrifuged at 8,000 rpm for 20 min and resuspended with 20 ml binding buffer. Then, the suspension cells were crushed by ultrasonication, followed by centrifugation at 12,000 rpm and 4°C for 20 min to prepare crude enzyme solution. Protein samples (10 μ l) were mixed with 10 μ l loading buffer and boiled for 10 min before performing SDS-PAGE. For SDS-PAGE, the stacking gel was comprised of 0.5 ml stacking buffer, 0.67 ml 30% acrylamide, 50 μ l 10% ammonium persulfate, 50 μ l 10% *N,N,N',N'*-tetramethylethylenediamine (TEMED), and 2.7 ml ddH₂O, and the separation gel was composed of 2.5 ml separation buffer, 4 ml 30% acrylamide, 0.1 ml SDS, 0.1 ml 10% ammonium persulfate, 50 μ l 10% TEMED, and 3.3 ml ddH₂O.

Analytical methods to determine nicotine metabolism characteristics. The growth profile and degradation ability of the wild type and gene knockout mutants were examined in BSM with nicotine. Strains were activated in LB medium and recultured to the logarithmic phase by monitoring OD₆₀₀ using a UV-2550 spectrophotometer; a 2% (vol/vol) inoculation amount was used for 100 ml BSM plus nicotine. OD₆₀₀ was detected every 6 h, and supernatant was harvested to determine residual nicotine concentration. The concentration of residual nicotine was determined by using high-performance liquid chromatography (HPLC) (1260 series; Agilent), then recording and comparing the sample peak areas and retention times. For HPLC analysis, samples were centrifuged at 12,000 rpm and 4°C for 15 min and harvested through a 0.22- μ m filter. An Agilent SB-C₁₈ column was involved in the HPLC-driven system, and the detector wavelength was set as 254 nm. The mobile phase was composed of methanol and 0.1 M KH₂PO₄ (pH 3.0), with a volumetric ratio of 10:90 (vol/vol), of which the flow rate was 1 ml/min. The retention time of nicotine is about 2.3 min according to the standard chemical information. All experiments were conducted in at least triplicate replicates, and the noninoculated BSM was taken as the negative control.

Intermetabolite identification of SP and NA using LC-MS detection methods. Resting cells of *P. putida* S-1 and its derivatives were used in this experiment to determine whether JY-Q-*NicAB* could transform SP or NA. Strains were activated and recultured to the logarithmic phase, then centrifuged at 5,000 rpm for 5 min and washed three times with PBS. Finally, they were resuspended with PBS to an identical optical density and treated overnight at 4°C to prepare resting cells. The final prepared concentration of NA was 1 mg/ml. SP was dissolved in methanol and added into the resting cells to a final concentration of 1 mg/ml. The reaction mixture was incubated at 180 rpm and 30°C for 2 days. Samples obtained after the reaction were treated with lysozyme for 30 min at 37°C, then centrifuged at 12,000 rpm for 15 min and harvested through a 0.22- μ m filter for subsequent LC-MS analysis. The intermediate metabolites were characterized with the LCQ Deca XP Plus LC-MS instrument (Thermo). Parallel samples were ionized by the electrospray circuiting positive polarity. The analysis parameters were set as the manufacturer recommended, and the mobile phase was prepared using a methanol-H₂O mixture (10:90, vol/vol) supplemented with 8 mM formic acid (23).

Statistical and bioinformatic methods. Statistical analysis was conducted with the GraphPad 6.0 program. One-way analysis of variance (ANOVA) was performed to detect statistical significance (*,

TABLE 2 Primers for RT-qPCR and gene knockout

Primer pair ^a	Sequences (5'–3') ^b	Product length (bp)
Primers for RT-qPCR		
16S-F, 16S-R	CACACTGGAAGTACGACACG, TGCTTTACAATCCGAAGACC	127
qspmA1-F, qspmA1-R	AACGTGCCAGTTTCCGTA, TGAAGTCAAGCAATCACCAGT	122
qspmA2-F, qspmA2-R	ACACCACCATGGAAACCGAA, CGGCTGGAATGGAAGGTGAA	106
qsirA2-F, qsirA2-R	GGCGAAAGTGCGGAAGTCCG, ACTGCTCAAGGCCAAGATGGA	103
qald1-F, qald1-R	TGCTGGCGGTGGATGAAT, CTTGCCTGTGAATGGCTTCC	155
qald2-F, qald2-R	CAGCCAGTTTCGCTGGATT, TCTTCGTTCGCGAGGCT	168
Primers for gene knockout		
spm1-UF, spm1-UR	ctatgacatgattacgaattcGCAACTGCGATGACAAGGCT, ttagcccagCCAATCTCTGTAGATTTTATGGAAGATT	459
spm1-DF, spm1-DR	cagagattggCTGGCTAAATCTCTGCAATG, caggtgactctagagatccGGGCGTGATTTCGTAGAGCG	524
spm2-UF, spm2-UR	ctatgacatgattacgaattcACAACCTTTGCGGTCTGC, cagcattgcaTTGCGCAAGACTCAAAGCCA	450
spm2-DF, spm2-DR	tccttgcgcaTGCAATGCTGGTCTTAACGT, caggtgactctagagatccGAGCGAAACCTTGAGCAATC	532
sirA2-UF, sirA2-UR	gagctcgtatcccggtatccGCATCAAGTCGACGAGAACT, ctgctgCTTTTCCAAGGATCGTCAATG	1,383
sirA2-DF, sirA2-DR	atccttggaaaagacCGCAGGCTCTCAAAGGC, acgacgcccagtgccaagcttGGTTACGGGTGTCGGCAAT	873
ald1-UF, ald1-UR	gagctcgtatcccggtatccGCTACCGTATTCCGCGGTAA, tgagccGGCTTTCTCCGGGTCTCG	724
ald1-DF, ald1-DR	acccggagaaagccGGCTCAGCGGCGCAAGCC, acgacgcccagtgccaagcttTGGCAGTGTGGCTATCTGGC	682
ald2-UF, ald2-UR	gagctcgtatcccggtatccTGGCTTCGAGACGAGATTG, ttgtgcgaTCAGGCTTGCTCCCCCTG	771
ald2-DF, ald2-DR	agcaagcctgaTCGCACAAGGGACGCCTC, acgacgcccagtgccaagcttCTGTATCCAGCGCCTTTTC	695
Verification primers for gene knockout		
yz-spm1-F, yz-spm1-R	CCGCCCTTTAGTGCAATTT, TTTCAGGTGCGACTCCCGAA	1,408
yz-spm2-F, yz-spm2-R	CCGTTTATCCCTAGCACCTC, AAAGATGCCACGCCTCCAAT	1,615
yz-sirA2-F, yz-sirA2-R	CAGCAGGTGGTGGTGTACTT, CGATTTGCCAGGTTGTAG	2,674
yz-ald1-F, yz-ald1-R	ATTTCCACCGCCGTTCA, AACGCACCTGTCCGATAACC	1,947
yz-ald2-F, yz-ald2-R	ATGTTCTCGGCGAGTTCGAC, TAGCGATTCCGCTGGTATT	1,999
Primers for gene expression		
nicAB-CF, nicAB-CR	gtcgcaggtatcgataagcttgaATGCAAACAACCGTCTCCCTG, cgctctagaactagtgatccTCAGTGGCTGCC AGGGTTG	4,034
ald2-CF, ald2-CR	gtcgcaggtatcgataagcttgaATGGAACACTACGCATCAACCAGAA, cgctctagaactagtgatccTCAGCTGAAG GTGTGGCGG	2,711
nicAB-yzF, nicAB-yzR	GTGTGGTCAAGTACGCAGAA, TGGTGGACTGGATGACGTTG	889

^aPrimer designations are based on the *Pseudomonas* sp. strain JY-Q genome (GenBank accession number CP011525).

^bUnderlined nucleotide abbreviations indicate restriction cleavage sites, and lowercase nucleotide abbreviations indicate homologous segments for plasmid-bearing sequences.

$P < 0.05$; **, $P < 0.01$; ***, $P < 0.001$). All data are shown as the mean plus or minus standard error (SE), with triplicate independent experiments. Sequence alignments were conducted using MUSCLE (44) and BLASTp (45).

Data availability. The genome sequence of *Pseudomonas* sp. JY-Q has been archived in GenBank under accession number CP011525.

ACKNOWLEDGMENTS

This work was financially supported by grants from the National Natural Science Foundation of China (no. 31970104, 31670115, and 31800118) and by the China Postdoctoral Science Foundation (grant 2017M621965).

We are grateful to Ning-Yi Zhou for constructive discussion.

We declare no conflict of interest.

No studies with human participants or animals were performed by any of the authors.

REFERENCES

- Mihasan M, Brandsch R. 2013. pAO1 of *Arthrobacter nicotinovorans* and the spread of catabolic traits by horizontal gene transfer in gram-positive soil bacteria. *J Mol Evol* 77:22–30. <https://doi.org/10.1007/s00239-013-9576-x>.
- Igloi GL, Brandsch R. 2003. Sequence of the 165-kilobase catabolic plasmid pAO1 from *Arthrobacter nicotinovorans* and identification of a pAO1-dependent nicotine uptake system. *J Bacteriol* 185:1976–1986. <https://doi.org/10.1128/jb.185.6.1976-1986.2003>.
- Li J, Wang J, Li S, Yi F, Xu J, Shu M, Shen M, Jiao Y, Tao F, Zhu C, Zhang H, Qian S, Zhong W. 2019. Co-occurrence of functional modules derived from nicotine-degrading gene clusters confers additive effects in *Pseudomonas* sp. JY-Q. *Appl Microbiol Biotechnol* 103:4499–4510. <https://doi.org/10.1007/s00253-019-09800-4>.
- Tang H, Wang L, Wang W, Yu H, Zhang K, Yao Y, Xu P. 2013. Systematic unraveling of the unsolved pathway of nicotine degradation in

- Pseudomonas*. *PLoS Genet* 9:e1003923. <https://doi.org/10.1371/journal.pgen.1003923>.
5. Huang H, Yu W, Wang R, Li H, Xie H, Wang S. 2017. Genomic and transcriptomic analyses of *Agrobacterium tumefaciens* S33 reveal the molecular mechanism of a novel hybrid nicotine-degrading pathway. *Sci Rep* 7:4813. <https://doi.org/10.1038/s41598-017-05320-1>.
 6. Yu H, Tang H, Zhu X, Li Y, Xu P. 2015. Molecular mechanism of nicotine degradation by a newly isolated strain, *Ochrobactrum* sp. strain SJY1. *Appl Environ Microbiol* 81:272–281. <https://doi.org/10.1128/AEM.02265-14>.
 7. Xia Z, Zhang W, Lei L, Liu X, Wei HL. 2015. Genome-wide investigation of the genes involved in nicotine metabolism in *Pseudomonas putida* J5 by Tn5 transposon mutagenesis. *Appl Microbiol Biotechnol* 99:6503–6514. <https://doi.org/10.1007/s00253-015-6529-x>.
 8. Li J, Qian S, Xiong L, Zhu C, Shu M, Wang J, Jiao Y, He H, Zhang F, Linhardt RJ, Zhong W. 2017. Comparative genomics reveals specific genetic architectures in nicotine metabolism of *Pseudomonas* sp. JY-Q. *Front Microbiol* 8:2085. <https://doi.org/10.3389/fmicb.2017.02085>.
 9. Li A, Qiu J, Chen D, Ye J, Wang Y, Tong L, Jiang J, Chen J. 2017. Characterization and genome analysis of a nicotine and nicotinic acid-degrading strain *Pseudomonas putida* JQ581 isolated from marine. *Mar Drugs* 15:156. <https://doi.org/10.3390/md15060156>.
 10. Li J, Shen M, Chen Z, Pan F, Yang Y, Shu M, Chen G, Jiao Y, Zhang F, Linhardt RJ, Zhong W. 2021. Expression and functional identification of two homologous nicotine dehydrogenases, NicA2 and Nox, from *Pseudomonas* sp. JY-Q. *Protein Expr Purif* 178:105767. <https://doi.org/10.1016/j.pep.2020.105767>.
 11. Tang H, Zhang K, Hu H, Wu G, Wang W, Zhu X, Liu G, Xu P. 2020. Molecular deceleration regulates toxicant release to prevent cell damage in *Pseudomonas putida* S16 (DSM 28022). *mBio* 11:e02012-20. <https://doi.org/10.1128/mBio.02012-20>.
 12. Yu H, Tang H, Xu P. 2014. Green strategy from waste to value-added-chemical production: efficient biosynthesis of 6-hydroxy-3-succinoyl-pyridine by an engineered biocatalyst. *Sci Rep* 4:5397. <https://doi.org/10.1038/srep05397>.
 13. Wang W, Xu P, Tang H. 2015. Sustainable production of valuable compound 3-succinoyl-pyridine by genetically engineering *Pseudomonas putida* using the tobacco waste. *Sci Rep* 5:16411. <https://doi.org/10.1038/srep16411>.
 14. Liu J, Ma G, Chen T, Hou Y, Yang S, Zhang KQ, Yang J. 2015. Nicotine-degrading microorganisms and their potential applications. *Appl Microbiol Biotechnol* 99:3775–3785. <https://doi.org/10.1007/s00253-015-6525-1>.
 15. Gurusamy R, Natarajan S. 2013. Current status on biochemistry and molecular biology of microbial degradation of nicotine. *ScientificWorldJournal* 2013:125385. <https://doi.org/10.1155/2013/125385>.
 16. Jimenez JL, Canales A, Jimenez-Barbero J, Ginalska K, Rychlewski L, Garcia JL, Diaz E. 2008. Deciphering the genetic determinants for aerobic nicotinic acid degradation: the *nic* cluster from *Pseudomonas putida* KT2440. *Proc Natl Acad Sci U S A* 105:11329–11334. <https://doi.org/10.1073/pnas.0802273105>.
 17. Jimenez JL, Juarez JF, Garcia JL, Diaz E. 2011. A finely tuned regulatory circuit of the nicotinic acid degradation pathway in *Pseudomonas putida*. *Environ Microbiol* 13:1718–1732. <https://doi.org/10.1111/j.1462-2920.2011.02471.x>.
 18. Yang Y, Yuan S, Chen T, Ma P, Shang G, Dai Y. 2009. Cloning, heterologous expression, and functional characterization of the nicotinate dehydrogenase gene from *Pseudomonas putida* KT2440. *Biodegradation* 20:541–549. <https://doi.org/10.1007/s10532-008-9243-x>.
 19. Xiao Y, Zhu W, Liu H, Nie H, Chen W, Huang Q. 2018. FinR regulates expression of *nicC* and *nicX* operons, involved in nicotinic acid degradation in *Pseudomonas putida* KT2440. *Appl Environ Microbiol* 84:e01210-18. <https://doi.org/10.1128/AEM.01210-18>.
 20. Brickman TJ, Armstrong SK. 2018. The *Bordetella bronchiseptica* *nic* locus encodes a nicotinic acid degradation pathway and the 6-hydroxynicotinate-responsive regulator BpsR. *Mol Microbiol* 108:397–409. <https://doi.org/10.1111/mmi.13943>.
 21. Guragain M, Jennings-Gee J, Cattelán N, Finger M, Conover MS, Hollis T, Deora R. 2018. The transcriptional regulator BpsR controls the growth of *Bordetella bronchiseptica* by repressing genes involved in nicotinic acid degradation. *J Bacteriol* 200:e00712-17. <https://doi.org/10.1128/JB.00712-17>.
 22. Jiang Y, Tang H, Wu G, Xu P. 2015. Functional identification of a novel gene, *moaE*, for 3-succinoylpyridine degradation in *Pseudomonas putida* S16. *Sci Rep* 5:13464. <https://doi.org/10.1038/srep13464>.
 23. Qiu J, Ma Y, Chen L, Wu L, Wen Y, Liu W. 2011. A *sirA*-like gene, *sirA2*, is essential for 3-succinoyl-pyridine metabolism in the newly isolated nicotine-degrading *Pseudomonas* sp. HZN6 strain. *Appl Microbiol Biotechnol* 92:1023–1032. <https://doi.org/10.1007/s00253-011-3353-9>.
 24. Qiu J, Ma Y, Wen Y, Chen L, Wu L, Liu W. 2012. Functional identification of two novel genes from *Pseudomonas* sp. strain HZN6 involved in the catabolism of nicotine. *Appl Environ Microbiol* 78:2154–2160. <https://doi.org/10.1128/AEM.07025-11>.
 25. Qiu J, Ma Y, Zhang J, Wen Y, Liu W. 2013. Cloning of a novel nicotine oxidase gene from *Pseudomonas* sp. strain HZN6 whose product nonenantioselectively degrades nicotine to pseudooxynicotine. *Appl Environ Microbiol* 79:2164–2171. <https://doi.org/10.1128/AEM.03824-12>.
 26. Xia Z, Lei L, Zhang HY, Wei HL. 2018. Characterization of the ModABC molybdate transport system of *Pseudomonas putida* in nicotine degradation. *Front Microbiol* 9:3030. <https://doi.org/10.3389/fmicb.2018.03030>.
 27. Yu H, Tang H, Li Y, Xu P. 2015. Molybdenum-containing nicotine hydroxylase genes in a nicotine degradation pathway that is a variant of the pyridine and pyrrolidine pathways. *Appl Environ Microbiol* 81:8330–8338. <https://doi.org/10.1128/AEM.02253-15>.
 28. Hu H, Wang L, Wang W, Wu G, Tao F, Xu P, Deng Z, Tang H. 2019. Regulatory mechanism of nicotine degradation in *Pseudomonas putida*. *mBio* 10:e00602-19. <https://doi.org/10.1128/mBio.00602-19>.
 29. Li J, Tai C, Deng Z, Zhong W, He Y, Ou HY. 2018. VRprofile: gene-cluster-detection-based profiling of virulence and antibiotic resistance traits encoded within genome sequences of pathogenic bacteria. *Brief Bioinform* 19:566–574. <https://doi.org/10.1093/bib/bbw141>.
 30. Li J, Yao Y, Xu HH, Hao L, Deng Z, Rajakumar K, Ou HY. 2015. SecReT6: a web-based resource for type VI secretion systems found in bacteria. *Environ Microbiol* 17:2196–2202. <https://doi.org/10.1111/1462-2920.12794>.
 31. El-Gebali S, Mistry J, Bateman A, Eddy SR, Luciani A, Potter SC, Qureshi M, Richardson LJ, Salazar GA, Smart A, Sonnhammer ELL, Hirsh L, Paladín L, Piovesan D, Tosatto SCE, Finn RD. 2019. The Pfam protein families database in 2019. *Nucleic Acids Res* 47:D427–D432. <https://doi.org/10.1093/nar/gky995>.
 32. Potter SC, Luciani A, Eddy SR, Park Y, Lopez R, Finn RD. 2018. HMMER web server: 2018 update. *Nucleic Acids Res* 46:W200–W204. <https://doi.org/10.1093/nar/gky448>.
 33. lobbi-Nivol C, Leimkuhler S. 2013. Molybdenum enzymes, their maturation and molybdenum cofactor biosynthesis in *Escherichia coli*. *Biochim Biophys Acta* 1827:1086–1101. <https://doi.org/10.1016/j.bbabbio.2012.11.007>.
 34. Chen DZ, Sun YM, Han LM, Chen J, Ye JX, Chen JM. 2016. A newly isolated *Pseudomonas putida* S-1 strain for batch-mode-propanethiol degradation and continuous treatment of propanethiol-containing waste gas. *J Hazard Mater* 302:232–240. <https://doi.org/10.1016/j.jhazmat.2015.09.063>.
 35. Chen DZ, Zhao XY, Miao XP, Chen J, Ye JX, Cheng ZW, Zhang SH, Chen JM. 2018. A solid composite microbial inoculant for the simultaneous removal of volatile organic sulfide compounds: preparation, characterization, and its bioaugmentation of a biotrickling filter. *J Hazard Mater* 342:589–596. <https://doi.org/10.1016/j.jhazmat.2017.08.079>.
 36. Brandsch R. 2006. Microbiology and biochemistry of nicotine degradation. *Appl Microbiol Biotechnol* 69:493–498. <https://doi.org/10.1007/s00253-005-0226-0>.
 37. Li H, Li X, Duan Y, Zhang KQ, Yang J. 2010. Biotransformation of nicotine by microorganism: the case of *Pseudomonas* spp. *Appl Microbiol Biotechnol* 86:11–17. <https://doi.org/10.1007/s00253-009-2427-4>.
 38. Zhong W, Zhu C, Shu M, Sun K, Zhao L, Wang C, Ye Z, Chen J. 2010. Degradation of nicotine in tobacco waste extract by newly isolated *Pseudomonas* sp. ZUTSKD. *Bioresour Technol* 101:6935–6941. <https://doi.org/10.1016/j.biortech.2010.03.142>.
 39. Shao Y, Li J, Wang Y, Yi F, Zhang Y, Cui P, Zhong W. 2019. Comparative genomics and transcriptomics insights into the C₁ metabolic model of a formaldehyde-degrading strain *Methylobacterium* sp. XJLW. *Mol Omics* 15:138–149. <https://doi.org/10.1039/c8mo00198g>.
 40. Medema MH, Takano E, Breitling R. 2013. Detecting sequence homology at the gene cluster level with MultiGeneBlast. *Mol Biol Evol* 30:1218–1223. <https://doi.org/10.1093/molbev/mst025>.
 41. Liu T, Li J, Qiu L, Zhang F, Linhardt RJ, Zhong W. 2020. Combined genomic and transcriptomic analysis of dibutyl phthalate metabolic pathway in *Arthrobacter* sp. ZJUTW. *Biotechnol Bioeng* 117:3712–3726. <https://doi.org/10.1002/bit.27524>.
 42. Zhou Z, Liu Y, Zanolli G, Wang Z, Xu P, Tang H. 2019. Enhancing bioremediation potential of *Pseudomonas putida* by developing its acid stress tolerance with glutamate decarboxylase dependent system and global

- regulator of extreme radiation resistance. *Front Microbiol* 10:2033. <https://doi.org/10.3389/fmicb.2019.02033>.
43. Zhang H, Zhao R, Huang C, Li J, Shao Y, Xu J, Shu M, Zhong W. 2019. Selective and faster nicotine biodegradation by genetically modified *Pseudomonas* sp. JY-Q in the presence of glucose. *Appl Microbiol Biotechnol* 103:339–348. <https://doi.org/10.1007/s00253-018-9445-z>.
 44. Edgar RC. 2004. MUSCLE: multiple sequence alignment with high accuracy and high throughput. *Nucleic Acids Res* 32:1792–1797. <https://doi.org/10.1093/nar/gkh340>.
 45. Camacho C, Coulouris G, Avagyan V, Ma N, Papadopoulos J, Bealer K, Madden TL. 2009. BLAST+: architecture and applications. *BMC Bioinformatics* 10:421. <https://doi.org/10.1186/1471-2105-10-421>.